Correlations and Ostwald ripening

M. Marder*
Department of Physics, University of California, Santa Barbara, Santa Barbara, California 93106
(Received 12 January 1987)

This paper examines the effect of diffusive interactions, and the correlations they create between particles, on Ostwald ripening. The effect accounts for a persistent discrepancy between theory and experiment, in which the distribution of particle sizes has been more broad and flat than mean-field theory predicts. A new model system is proposed to study the problem, and a hierarchy of equations derived from it is expanded in powers of the square root of the volume fraction. The time devlopment of correlations is analyzed through an unusual perturbation theory. The resulting differential equations are solved numerically and compared with experiment.

I. INTRODUCTION

If a mixture of aluminum and nickel is raised above 1600 °C the metals are molten and may be stirred together in any amount. Below approximately 1200 °C they solidify and begin to separate. If only a small portion of the mixture is nickel, then nickel will begin to form into tiny droplets of Ni_3Al dispersed fairly uniformly in a background of aluminum. This behavior is common in a wide variety of alloys, as well as in binary liquids. The metals are not in equilibrium as they are not completely separated. The true equilibrium state of the alloy consists of a block of nickel sitting next to a block of aluminum, but thousands of trillions of years would be required even for one cubic centimeter of material to reach true equilibrium.

Two factors contribute to the length of approach to equilibrium. Most important is the fact that for regions of solid nickel to accumulate, nickel atoms must diffuse through the aluminum surrounding them, and diffusion in solids at low temperatures is very slow. More subtle is the competition between surface and volume energies. Although large regions of nickel are thermodynamically advantageous, interfaces between nickel and aluminum are disadvantageous, so that regions with large surface-to-volume ratios, such as small particles, may be unstable. In fact, once nucleation has produced a collection of nickel droplets in aluminum, one watches their time evolution and sees large ones grow while small ones shrink. A theory first published by Lifshitz and Slyozov[1,2] in 1958 predicts that after long times the distribution of droplet sizes, properly scaled, should reach a universal form that is independent of all materials parameters. Qualitative features of this theory have been confirmed,[3] but as shown in Fig. 1 measured particle size distributions are more broad and squat[4–12] than the prediction of Lifshitz and Slyozov.

The origin of discrepancies between theory and experiment in this process, known as Ostwald coarsening,[13] has been difficult to trace, in part because the magnitude of the disagreement is not especially dramatic, and in part because many scenarios might be conjured up to explain the observations. One review article[14] suggests no less than six separate phenomenological models. We will see that interactions between particles, of a sort first proposed by Weins and Cahn,[15] are sufficient to explain the effect. A new asymptotic theory developed here focuses on correlations that build up between particles in the long-time limit, and finds that particle size distributions should depend substantially upon the volume fraction of precipitate, even for volume fractions as low as 1%. The theory may be useful in determining materials parameters such as surface tensions or low-temperature diffusion rates that now are difficult to measure.

Metals which contain small spheres of a second phase are of some practical importance. The spheres serve to trap dislocations, increasing the strength of the metal, and unlike diffuse clouds of impurities, they do not easily become mobile as the temperature of the alloy increases. In choosing an optimum size for the spheres, so that the metal may be as strong as possible, two considerations need to be kept in mind. If the spheres are small, dislocations can cut through them under sufficient applied stress, and the metal will yield in this way. On the other hand, for a given amount of second-phase material, if the size of

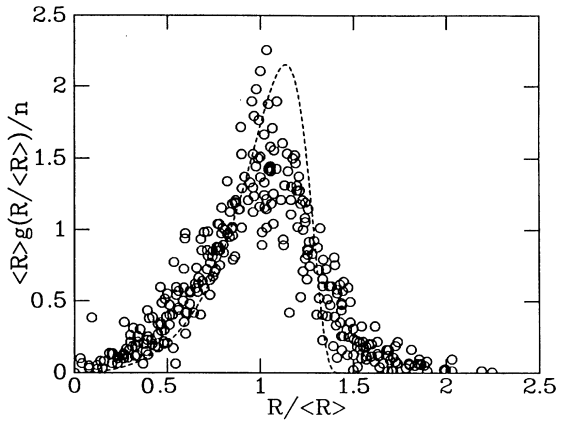

FIG. 1. 20 years of experiments, Refs. 4–12, indicate that particle size distributions are broader than predicted by the mean-field theory of Lifshitz and Slyozov.

the droplets increases, the spacing between them increases and the dislocations can more easily slip between the spheres altogether. Reviews of these processes may be found in Refs. 16 and 17. In practice, one wants spheres of approximately 100 Å separated at a mean distance of 1000 Å for greatest metallic strength.[18] However, a metal created in this way will not remain so forever, as it is not in equilibrium; and when the spheres within it grow, its strength will decrease. The time scales on which this process occurs will occupy the remainder of this paper.

A brief sketch of the work described here has already been published.[19] In Sec. II. I will motivate a model to study the growth and competition of spheres. It is a modification of a model introduced by Weins and Cahn,[15] rediscovered by Kawasaki and Ohta,[20] and first investigated systematically by Tokuyama, Kawasaki, and Enomoto.[21–24] The slight changes made here allow one to study the complete time evolution of the system, rather than simply late-stage scaling behavior. Then various average quantities of physical interest will be computed to first order in the square root of the volume fraction. At this point, one has closed equations describing the time evolution of two-particles correlations in the system. Unfortunately, the two-particle correlation functions involve three variables, plus time, and numerical solutions of the equations at this point would be difficult. By analyzing the way that correlation develop, we will find simpler equations for them. The resulting expressions are solved numerically and compared with experiment, alternate numerical procedures, and previous theories.

II. CORRELATED DYNAMICS

A. The starting model

Let us consider an idealized dilute binary alloy or binary liquid at any time after the end of nucleation. It consists of many perfectly spherical droplets of minority phase embedded in a background of two-phase material. We will assume that the spheres do not move, that their centers are always fixed. Some of the errors involved in this assumption are examined in Appendix A. In solids the assumption is sensible, but in liquids it may not be.

Outside of each droplet, if it grows slowly enough, the assumption of local equilibrium gives the Gibbs-Thomson condition[25,26]

$$\Phi(r_i,t)=\frac{d_0}{R_i} . \tag{2.1}$$

Here $\Phi(r,t)$ is the concentration, say, of nickel as a function of space and time, d_0 is a capillary length related to surface tension,[27,28] and r_i is any point on the outside surface of the ith droplet which is of radius R_i. Concentrations will be measured in volume percent. Between droplets we must satisfy the diffusion equation

$$\frac{\partial\Phi}{\partial t}=D\nabla^2\Phi . \tag{2.2}$$

Growth of the droplets is assumed to be limited only by the ability of diffusion to bring material to their surfaces. Since the droplets always remain spheres,

$$\frac{d}{dt}\frac{4\pi}{3}R_i^3=\int_{S_i} d^2S\,\mathbf{n}\cdot D\nabla c , \tag{2.3}$$

where the integral is taken over the surface of the ith droplet, and $\hat{\mathbf{n}}$ is a unit normal pointing out of the droplet.

Despite the many simplifications that have already been employed, when as few as two droplets are present, exact solution of the diffusion equation becomes a formidable task, only possible numerically,[29] and when millions of droplets are present, even numerical solution is out of the question. However, the full diffusion equation may be solved exactly for one droplet if it is so large that the Gibbs-Thomson condition (2.1) may be approximated by

$$\Phi(r_i,t)=0 .$$

In this case a result due to Zener[30] states that

$$\Phi(\mathbf{r},t)=\Phi_\infty-c\left[\frac{r}{l(t)}\right]\Big/c\left[\frac{R}{l(t)}\right] ,$$

where Φ_∞ is a constant concentration at infinity, $R(t)$ obeys

$$R(t)=\lambda(Dt)^{1/2} ,$$

for some constant λ which matches the boundary conditions,

$$l(t)=(2Dt)^{1/2} ,$$

and

$$c(x)=\int_x^\infty \frac{e^{-z^2/2}}{z^2}dz .$$

These equations simplify when Φ_∞ is much less than one. To first order in Φ_∞ and for $R\ll l$ we will have

$$\Phi(\mathbf{r},t)=\Phi_\infty+Q\frac{e^{-r^2/2l^2}}{r} ,$$

with $Q=-R^2\dot{R}/D$. Q is chosen correctly since the gradient of the concentration at the surface of the droplet is Φ_∞/R, and the drop thus grows at the rate

$$\dot{R}=\Phi_\infty\frac{D}{R}\Rightarrow R=(\Phi_\infty)^{1/2}l .$$

The concentration field described here decays as $1/r$ and is time independent for $r\ll 1$; but at greater distances, it falls off very rapidly.

Let us now proceed to construct an approximate solution to the full diffusion equation (2.2) satisfying the boundary condition (2.1) for N droplets, in the form

$$Q_i=\frac{-R_i^2\dot{R}_i}{D} , \tag{2.4}$$

$$\Phi(r,t)=\Phi_\infty(t)+\sum_{i=1}^{N}Q_i(t)\frac{e^{-|\mathbf{r}_i-\mathbf{r}|^2/2l^2}}{|\mathbf{r}_i-\mathbf{r}|} . \tag{2.5}$$

If droplets are scattered very sparsely throughout the system, then they should become independent and a sum of the form (2.5) should become exact. (2.5) does not have sufficient freedom to satisfy (2.1) for all particles exactly;

however, the boundary condition is approximately satisfied if

$$d_0/R_i=\Phi_\infty(t)+\frac{Q_i}{R_i}+\sum_{j(\neq i)}Q_j\frac{e^{-|\mathbf{r}_i-\mathbf{r}_j|^2/2l^2}}{|\mathbf{r}_i-\mathbf{r}_j|} . \quad (2.6)$$

This approximation ignores terms of order $(R_i/|\mathbf{r}_i-\mathbf{r}_j|)^2$. In order to fix Φ_∞, we will require that solute be conserved. The amount of material contained in a single droplet is $(4\pi/3)R^3$ so that all the droplets in a box of volume Ω contain an amount of material per unit volume

$$\phi=\sum_i\frac{4\pi}{3}\frac{R_i^3}{\Omega} .$$

The diffusion field coming from a single droplet contains an amount of material $4\pi l^2Q_i$ according to (2.5). Defining $\langle Q\rangle=\sum_{i=1}^N Q_i/N$, the volume fraction of solute not yet contained in droplets is

$$\Delta\equiv\phi_f-\phi=\Phi_\infty(t)+4\pi nl^2\langle Q\rangle , \quad (2.7)$$

where ϕ_f equals both the initial supersaturation and the volume fraction of the minority phase once the phase transition has gone to completion, as concentration is measured in volume percent. Equations (2.5) and (2.6) were first written down by Weins and Cahn,[15] although in their treatment $l\to\infty$. Kawasaki and Ohta[20] later rediscovered the equation of Weins and Cahn. The reader may wonder whether including $l=(2Dt)^{1/2}$ does not unnecessarily complicate matters. We will see presently that l does not enter into any final equation of physical interest. However, that does not mean that it may be omitted entirely. The diffusion length l is a residue of the complicated time-dependent behavior of diffusion fields outside of droplets and serves to cut off otherwise infinite-range interactions between particles in a physically sensible manner. The form of the cutoff is irrelevant, as one should hope, since one cannot compute it precisely, but if it is absent, we shall see that the physical content of the model changes.

To examine the conditions under which the approximations leading to (2.6) are valid is a difficult task which requires separate consideration of many different points. Some of these matters are considered in Appendix A which calculates one particular sort of correction to (2.6) and shows it to be negligible. For the moment, let us note that $\phi\ll 1$ is a necessary condition. Suppose that two droplets of radius R have centers a distance $2R$ apart. Then we have found a case in which $R/|\mathbf{r}_i-\mathbf{r}_j|$ is not small, so the approximations leading to (2.6) begin to fail. However, if one chooses one droplet at random, the number of additional droplets within a sphere of radius $2R$ surrounding it is $(32\pi/3)nR^3\sim 8\phi$, and if ϕ is very small, the chances of finding two droplets close together become correspondingly small. If all corrections to the Lifshitz-Slyozov mean-field theory were of order ϕ, we should have to calculate effects due to very nearby droplets; as droplets react to each other in a very nonlinear way, that would be difficult. The crucial simplification in this problem occurs because there arise corrections to the Lifshitz-Slyozov theory at order $(\phi)^{1/2}$ which dominate when the volume fraction ϕ is small, and allow one to neglect terms of order ϕ. In order to understand the manner in which they appear, one should appreciate the significance of a new length scale in the problem, the screening length, whose importance was first recognized by Marqusee and Ross.[31]

Notice that (2.6) describes a set of conducting spheres with a potential at the surface of each sphere given by (2.1). Let us examine the length over which interactions decay in a very similar but slightly simpler system. Consider a collection of N conducting spheres of radius R, each maintained at zero potential, and placed randomly in a volume Ω as pictured in Fig. 2. So that the potential will not simply be zero throughout all space, add a single point charge at the origin. Consider a volume of size Ω/N surrounding one of the spheres, and label the location of this whole volume with the coarse-grained position variable x. Away from the sphere, but still within this volume, the electrostatic potential $\Phi(r)$ goes to some nearly constant value $\Phi_\infty(x)$. However, on the surface of the sphere, $\Phi=0$, so Φ must locally be of the form

$$\Phi(r)=\Phi_\infty(x)-\frac{\Phi_\infty(x)R}{r} ,$$

choosing $r=0$ at the center of the sphere. Thus a charge $Q(x)=-\Phi_\infty R$ is induced on the surface of the sphere. In the space between between spheres Laplace's equation holds but to consider all of space, we must write

$$\nabla^2\Phi(r)=-4\pi\rho(r) ,$$

where ρ is the charge density. Average this last equation over the positions of the spheres. The average value of $\Phi(r)$ in the box located by x is $\Phi_\infty(x)$ so long as $\Omega/N\gg R^3$, and the charge density in the same box is $Q(x)n=-\Phi_\infty(x)Rn$. Remembering the point charge at the origin, we now have

$$\nabla^2\Phi_\infty(x)=4\pi[nR\Phi_\infty(x)-\delta(x)] ,$$

which one may easily solve to obtain

$$\Phi_\infty(x)=\frac{e^{-x/\xi}}{x} ,$$

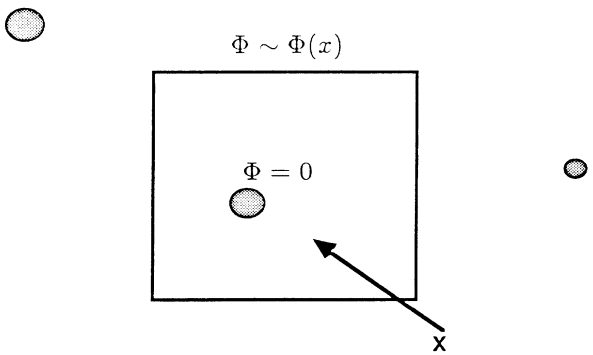

FIG. 2. At each of these well-separated metal spheres the potential Φ goes to zero, but in between them it goes to a slowly varying value $\Phi(x)$, where x labels the whole box surrounding one of the particles.

with

$$\xi=(4\pi nR)^{-1/2} .$$

ξ arises naturally in a formal analysis, but its physical origin is most clear in the present simple case. (2.6) is identical to an equation of electrostatics only for $\mathbf{r}_i-\mathbf{r}_j \ll l$, so for the analysis above to apply consistently to it, one must have $\xi \ll l$. One may always assume $\xi \ll l$ for a simple reason. Immediately after nucleation, it may be true that in fact $\xi > l$. However, we will see that ξ enters into all equations only by multiplying terms in the dimensionless combination $\langle R \rangle /\xi$. Since $\langle R \rangle$ is always much less than l, the distance over which diffusion has acted since the particles were formed, terms containing ξ are only considerable if $\xi \ll l$. No error results if one simply assumes this inequality to hold at all times.

B. Statistical preliminaries

Before proceeding to a formal treatment, let us establish why correlations among droplets should be important. Suppose that we examine our system and find a small droplet. The reason it has become small is that its neighborhood contains relatively large droplets which have competed with it for material. Therefore, not only is the droplet small, but it is shrinking more quickly than a mean-field treatment would lead one to expect. Similarly, large droplets should typically be growing more quickly than a theory without correlations could explain. As a result, size distributions are substantially broadened by the presence of correlations. We have already established that the probability of finding two droplets separated by a distance on the order of typical particle radii is small, of order ϕ. The probability of finding particles separated by a distance ξ, conversely, is large, and diverges as $\phi \to 0$. The important interactions will turn out to be between particles separated by this typical length. One may estimate the order of the interactions as follows: On the average particles have a "charge" $\langle Q \rangle$. This average value leads to the growth law of Lifshitz and Slyozov. If we insert a new particle into the system, of charge Q and radius R, it will alter the charges on other particles up to a distance ξ. The amount it will alter the charge on a particle at distance r, according to (2.6), is of order QR/r. The resulting effect of interaction back upon the particle we have just added is of order $Q(R/r)^2$. The important length of interactions is ξ and there are $n\xi^3$ particles in a volume of this radius. Therefore, the alteration in charge of the particle at the origin due to interactions is $n\xi^3(R^2/\xi^2)Q \sim QR/\xi \sim Q(\phi)^{1/2}$. This argument demonstrates the origin of terms of order $(\phi)^{1/2}$. That $(\phi)^{1/2}$ is the important expansion parameter was first pointed out by Tokuyama and Kawasaki.[21]

In order to complete the analogy with electrostatics that is suggested by Eqs. (2.5) and (2.6), now define

$$\rho(\mathbf{r})=\sum_{i=1}^{N} Q_i \delta(\mathbf{r}-\mathbf{r}_i) . \tag{2.8}$$

ρ bears no direct relationship to the concentration field Φ, and might be regarded as a generating functional for the Q's, or as a fictitious charge density. The dynamical equations (2.6) written in terms of ρ become

$$Q_j=d_0-\Phi_\infty R_j-R_j \int' d^3r\rho(\mathbf{r})\frac{e^{-|\mathbf{r}j-\mathbf{r}|^2/2l^2}}{|\mathbf{r}_j-\mathbf{r}|} . \tag{2.9}$$

where the prime over the integral indicates that one must remove the component of ρ which contains a δ function peaked at $\mathbf{r}_j$, just as one omits the term $i=j$ of the sum in (2.6). For example,

$$\int' d^3r\rho(\mathbf{r})\frac{e^{-|\mathbf{r}_1-\mathbf{r}|^2/2l^2}}{|\mathbf{r}_1-\mathbf{r}|} = \int d^3r[\rho(\mathbf{r})-\delta(\mathbf{r}-\mathbf{r}_1)Q_1]\frac{e^{-|\mathbf{r}_1-\mathbf{r}|^2/2l^2}}{|\mathbf{r}_1-\mathbf{r}|} . \tag{2.10}$$

A statistical treatment of the equations of motion for the droplets is most convenient and most intuitive in terms of this electrostic analogy.

Let us now establish the machinery needed for a statistical study of the model system. The ensemble we will adopt is based upon the assumption that at $t=0$, which we may take as the moment that nucleation ends, all particles are distributed at random. This assumption is surely incorrect, for the location at which partlices nucleate is surely affected by the presence or absence of other particles. However, these correlations are not the object of the present study, and as we will find that traces of initial conditions rapidly disappear, when particles grow and compete, the convenient assumption of initial uncorrelation should not lead to errors. A given experiment is not performed on an ensemble of initial conditions; one picks a certain initial configuration at random, allows it to evolve, and hopes that the results do not depend on initial conditions at all. The reason that one expects an average over initial conditions to mimic the behavior of a single system, is that one expects the system to be self-averaging. Regions farther apart than the screening length ξ do not communicate, and therefore grow independently. If a sample is sufficiently large, it consists of a large number of independent configurations, each of linear dimensions on the order of the screening length, and summing over these should be the same as summing over an ensemble of initial conditions. Let $R_1(t)R_2(t),\ldots,R_N(t)$ denote solutions of the deterministic problem in which N particles are placed at various time-independent locations, and allowed to evolve according to the growth law (2.6). Let $g_0(R_1^0,r_1^0;R_2^0r_2^0;\ldots;R_N^0,r_N^0)$ give the probability of finding particles $1,2,\ldots,N$ at locations $r_1^0r_2^0,\ldots,r_N^0$ with radii $R_1,R_2,\ldots,R_N$ at time $t=0$; we will assume g_0 to be symmetrical under permutations of particle labels. If Ω is the size of the system, then normalize g_0 by

$$\int dx_0 g_0(R_1^0,\ldots,r_N^0)=1 , \tag{2.11}$$

where

$$dx_0=\frac{d^3r_1^0}{\Omega}\frac{dR_1^0}{N}\cdots\frac{d^3r_N^0}{\Omega}\frac{dR_N^0}{N} . \tag{2.12}$$

The probability function of central importance is

$$g_N(R_1',r_1';R_2',r_2';\ldots;R_N',r_N':t) ,$$

which gives the probability of finding particles $1,2,\ldots N(t)$ at locations $r_1',r_2',\ldots r_N'$ at time t. It is given by

$$g_N(R_1',r_1';\ldots;R_N',r_N':t) = \int dx_0 g_0(R_1^0,\ldots,r_N^0) \times \prod_{k=1}^{N} [\delta(R_k'-R_k(t))\delta(r_k'-r_k^0)N\Omega] .$$

From g_N may be constructed all the averages of physical interest. Define

$$\langle A' \rangle = \int \prod_{k=1}^{N} \left[\frac{d^3 r_k'}{\Omega} \frac{dR_k'}{N} \right] g_N(R_1',r_1';\ldots;R_N',r_N':t) \times A'(R_1',r_1';\ldots;R_N',r_N') .$$

The integrals over $R_1',R_2',\ldots,R_N'$ must be taken from 0 to ∞, and the spatial integrals over the volume Ω. The one-particle distribution function $g_1(R_1,t)$, which gives the number of particles per volume of size R_1 at time t is defined by

$$g_1(R_1,t) = \langle \delta(R_1-R_1')\delta(\mathbf{r}_1-\mathbf{r}_1')N \rangle . \tag{2.13}$$

In the study of correlations, the two-particle function will be important, and that is defined by

$$g_2(R_1,R_2,r,t) = \left\langle \prod_{k=1}^{2} [\delta(R_k-R_k')\delta(\mathbf{r}_k-\mathbf{r}_k')N] \right\rangle . \tag{2.14}$$

This gives the probability of finding two particles of specified radii separated by a distance $r = |\mathbf{r}_1-\mathbf{r}_2|$. The treatment given here glosses over the fact that N varies in time and is not necessarily an integer. This technical point is treated properly in Ref. 28, but none of the complications change any of the following equations.

The final goal of these calculations will be the one-particle distribution function $g_1(R_1,t)$, which is usually measured in experiments. To find it we will allow it to evolve in time from initial conditions. Because of the deterministic evolution of g_N, any operator A' which vanishes for all $R_i'=0$, $R_3' \to \infty$, and does not depend on time explicitly, obeys the equation of motion

$$\frac{\partial}{\partial t}\langle A' \rangle = -\sum_{i=1}^{N} \frac{\partial}{\partial R_k} \langle A' \dot{R}_k(t) \rangle . \tag{2.15}$$

We will have as a boundary condition that $g_1(R_1,t)$ vanishes for $R_1=0$, and so we can write

$$\frac{\partial}{\partial t} g_1(R_1,t) = -\frac{\partial}{\partial R} v_1(1) g_1(R_1,t) , \tag{2.16}$$

where

$$v_1(1) = \frac{\langle \dot{R}_1' \delta(\mathbf{r}_1-\mathbf{r}_1')\delta(R_1-R_1')N \rangle}{g_1(R_1,t)} . \tag{2.17}$$

$v_1(1)$ gives the growth rate of particle 1 after averaging over all environments in which it might be located. When one observes a system of growing particles, singles out all those of radius R_1, measures their growth rates, and averages, the result is $v_1(1)$. Another interpretation of the averaging process is that particle 1 is held fixed at $\mathbf{r}_1$ while all other particles are "smeared out" into an effective background. It should be emphasized that (2.16) involves no approximations, so that if one calculates $v_1(1)$ exactly, one then may exactly compute $g_1(R_1,t)$. The argument of $v_1(1)$ indicates that we have not averaged over the position or size of particle 1, while the subscript indicates that we are looking at the growth rate of particle 1. Another example of this notation for averages is

$$Q_1(1,2) = Q_1(R_1,R_2,|\mathbf{r}_1-\mathbf{r}_2|) = \left\langle Q_1' \prod_{k=1}^{2} [\delta(\mathbf{r}_k-\mathbf{r}_k')\delta(R_k-R_k')N] \right\rangle \Big/ g_2(R_1,R_2,|\mathbf{r}_1-\mathbf{r}_2|) , \tag{2.18a}$$

which gives the charge [or growth rate using (2.4)] of particle 1 when both particles 1 and 2 are held fixed but all other particles have been smeared out.

$$\rho(1,2\,|\,\mathbf{r}) = \left\langle \rho'(r) \prod_{k=1}^{2} [\delta(\mathbf{r}_k-\mathbf{r}_k')\delta(R_k-R_k')N] \right\rangle \Big/ g_2(R_1,R_2,|\mathbf{r}_1-\mathbf{r}_2|) \tag{2.18b}$$

gives the charge density at $\mathbf{r}$ due to particles 1 and 2, if one averages over the locations of all others. In general, if I indicate explicitly a dependence upon the locations of particles 1 and 2 it means that all other particles have been averaged out.

To calculate $v_1(1)$ exactly from (2.17) would require knowledge of $\dot{R}_1$ for all possible configurations of particles. However, to compute it approximately requires only the knowledge of correlations and averages up to a certain order. The averaged growth rates and correlation functions I have defined are linked in a hierarchy. Truncating the hierarchy at first order recovers the equations of Lifshitz and Slyozov.[1] Truncating it at second order produces a set of equations that include all corrections to order $(\phi)^{1/2}$. To go beyond this level would be extremely difficult, for at order ϕ the growth law (2.6) and even the conservation law (2.7) acquire corrections, while the hierarchy becomes extremely complicated. The hierarchy

follows by performing averages on (2.8) and (2.9). Averaging (2.8) over the sizes and locations of all particles gives

$$\langle \rho \rangle = \sum_{i=1}^{N} \langle Q_i' \delta(\mathbf{r}-\mathbf{r}_1') \rangle$$

$$= \int dR_1 \langle \delta(R_1'-R_1)\delta(\mathbf{r}-\mathbf{r}_1')Q_1 N \rangle$$

$$= \int d^3r_1 dR_1 g_1(R_1,t) Q_1(1)\delta(\mathbf{r}-\mathbf{r}_1) = n\langle Q \rangle \ . \quad (2.19)$$

We may from now on place $\mathbf{r}_1$ at the origin, gaining some slight simplifications. Equation (2.19) has the interpretation that the average charge density equals the density of particles times the average charge upon them. In order to find $Q_1(1)$ average (2.9) over all particles but the first to obtain similarly

$$Q_1(1) = d_0 - \Phi_\infty R_1 - R_1 \int' d^3r \rho(1 \mid \mathbf{r}) \frac{e^{-r^2/2l^2}}{r} \ . \quad (2.20)$$

The next level of the hierarchy is

$$\rho(1 \mid \mathbf{r}) = Q_1(1)\delta(\mathbf{r}) + n \int d^3r_2 \frac{dR_2}{N} \frac{g_2(R_1,R_2,\mathbf{r}_2)}{g_i(R_1)} \times Q_2(1,2)\delta(\mathbf{r}-\mathbf{r}_2) \ , \quad (2.21)$$

$$Q_2(1,2) = d_0 - \Phi_\infty R_2 - R_2 \int' d^3r \rho(1,2 \mid \mathbf{r}) \frac{e^{-|\mathbf{r}_2-\mathbf{r}|^2/2l^2}}{|\mathbf{r}_2-\mathbf{r}|} \ . \quad (2.22)$$

C. Truncations

The next step is to recover the equations of Lifshitz and Slyozov by truncating at first order. To do this, we must find a sensible expression for $\rho(1 \mid \mathbf{r})$ in terms of functions which appear lower than it in the hierarchy. For $r \gg \xi$ the influence of particle 1 must become exponentially small, because of screening, and $\rho(1 \mid \mathbf{r})$ must approach a constant. Since the value of that constant cannot depend on the value $Q_1(1)$, it must be $\langle \rho \rangle$. We will try the approximation

$$\rho(1 \mid \mathbf{r}) \approx \langle \rho \rangle \ , \quad (2.23)$$

which is shown pictorially in Fig. 3. We expect $\rho(1 \mid \mathbf{r})$ to resemble the charge distribution surrounding a screened point charge, but are replacing it by its asymptotic value. Placing this into (2.20) gives

$$Q_1(1) = d_0 - \Phi_\infty R_1 - R_1 4\pi n l^2 \langle Q \rangle = d_0 - \Delta R_1 \ , \quad (2.24)$$

using the conservation law (2.7). From this calculation it should seem plausible that the precise form of the cutoff l does not matter, since precisely the same integral occurs here as in the calculation of solute conservation, and l therefore disappears from the problem. But we may also see why one cannot omit l altogether, sending it to infinity at the start of the calculation. For if one makes that choice, the conservation law (2.7) will imply $\langle Q \rangle = 0$, and (2.24) becomes $Q_1(1) = d_0 - \Phi_\infty R_1$; since $\langle Q \rangle = 0$, Φ_∞ is determined and $Q_1(1) = d_0(1 - R_1/\langle R \rangle)$. Thus sending $l \to \infty$ gives the starting equation of Wagner,[32] which only applies to the very late stage of growth. By sending $l \to \infty$ one constrains one's self to consider the asymptotic regime in which $\langle R \rangle$ equals d_0/Δ, whereas we will want to study the full-time development of the system. Equation (2.24) is equivalent to the growth law of Lifshitz and Slyozov, since $Q_i = R_i^2 v(R_i)/D$ implies

$$v_1(R_1) = \frac{D}{R_1}\left[\frac{\Delta}{R_1} - \frac{d_0}{R_1}\right] \ .$$

The generalization of this calculation to include two-body correlations proceeds in an analogous way. The first step is to find an approximation for $\rho(1,2 \mid \mathbf{r})$; the resulting equations may then be solved, and one may show by making a plausible guess about the structure of the neglected terms, that the errors incurred in the approximation are of order ϕ.

As an approximation for $\rho(1,2 \mid \mathbf{r})$ we will use

$$\rho(1,2 \mid \mathbf{r}) \approx [\rho(1 \mid \mathbf{r}) - \langle \rho \rangle] + [\rho(2 \mid \mathbf{r}) - \langle \rho \rangle] + \langle \rho \rangle \ . \quad (2.25)$$

This choice is illustrated in Fig. 4. It is the simplest way to ensure that when particles 1 and 2 are well separated, by a distance greater than ξ, and they become independent, the charge density assumes the proper asymptotic form and is exact to the level of one-particle functions. However, when the particles are within a screening length of one another, those interactions are ignored which cause the screening clouds to change their shape. Such interactions are three-body effects that are of order ϕ and therefore negligible.[28]

Inserting (2.25) into (2.22) closes the hierarchy. One finds immediately that

$$Q_2(1,2) = Q_2(2) - R_2 \int' d^3r_a [\rho(1 \mid \mathbf{r}_a) - \langle \rho \rangle] \frac{e^{-|\mathbf{r}_2-\mathbf{r}_a|^2/2l^2}}{|\mathbf{r}_2-\mathbf{r}_a|} \ .$$

Using (2.21) now gives

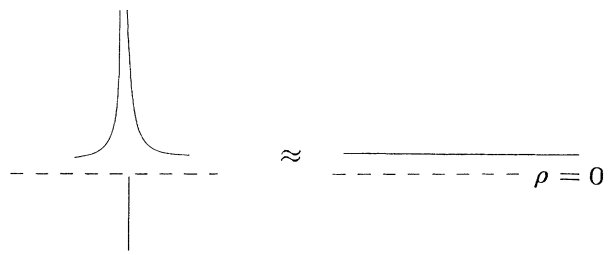

FIG. 3. To obtain the theory of Lifshitz and Slyozov, one approximates the charge distribution surrounding a screened point charge by its asymptotic value.

$$\rho(1\mid\mathbf{r})=Q_1(1)\delta(\mathbf{r})+n\langle Q\rangle+\rho_{\rm cr}(R_1,r)$$
$$-n\langle R\rangle\int d^3r_a[\rho(1\mid\mathbf{r})-\langle\rho\rangle]\frac{e^{-|\mathbf{r}_a-\mathbf{r}|^2/2l^2}}{|\mathbf{r}_a-\mathbf{r}|}$$
$$-\int d^3r_a\int dR_2\frac{G_2^c(R_1,R_2,|\mathbf{r}-\mathbf{r}_a|)}{g_1(R_1,t)}$$
$$\times R_2\frac{e^{-|\mathbf{r}_a-\mathbf{r}|^2/2l^2}}{|\mathbf{r}_a-\mathbf{r}|}[\rho(1\mid\mathbf{r})-\langle\rho\rangle]\ . \tag{2.26}$$

G_2 is the connected part of the two-particle correlation function defined by

$$G_2^c(R_1,R_2,r,t)=g_2(R_1,R_2,r,t)-\prod_{k=1}^{2}g_1(R_k,t)\ .$$

$\rho_{\rm cr}$ gives a contribution to the charge cloud surrounding each droplet as

$$\rho_{\rm cr}(r,R_1)=\int dR_2\frac{G_2^c(R_1,R_2,r)}{g_1(R_1,t)}Q_2(2)\ . \tag{2.27}$$

This term records the cumulative size changes that have been induced in nearby particles due to the presence of particle 1. The last term of (2.26) is of order ϕ and may be neglected. The demonstration relies on the fact that both correlations and charge clouds are modulated by a spatial dependence going as

$$\frac{\langle R\rangle e^{-r/\xi}}{r} \tag{2.28}$$

at long distances. That the connected piece of the two-point correlation function behaves in this way will be shown later. One must notice as well that two droplets cannot be closer together than the sum of their radii, so $G_2^c(R_1,R_2,r)$ vanishes for $r<R_1+R_2$. Elsewhere, this excluded-volume effect will be of order ϕ and therefore unimportant, but here it is necessary to prevent a possible logarithmic divergence in the integral at hand. Inserting the spatial dependence (2.28) for G_2^c and $\rho(1\mid\mathbf{r})-\langle\rho\rangle$, remembering the cutoff at small $r\le\langle R\rangle$, one can now show the term to be negligible. A fast way to do the estimate is to notice that since ξ is the important length scale, (2.28) is of order $\langle R\rangle/\xi\sim(\phi)^{1/2}$. The two factors of this term which appear in the last term of (2.26) make this term of order ϕ. An additional simplification results from the fact that soon after nucleation l grows so that $l\gg\xi$. l grows as $t^{1/2}$ and all other lengths in the problem grow as $t^{1/3}$ at late times. Since $\rho(1\mid\mathbf{r})-\langle\rho\rangle$ decays on a length scale ξ, sending $l\to\infty$ in (2.26), causes no error. To order $(\phi)^{1/2}$ we have

$$\rho(1\mid\mathbf{r})=Q_1(1)\delta(\mathbf{r})+n\langle Q\rangle+\rho_{\rm cr}(R_1,r)$$
$$-n\langle R\rangle\int d^3r_a\frac{[\rho(1\mid\mathbf{r}_a)-\langle\rho\rangle]}{|\mathbf{r}-\mathbf{r}_a|}\ .$$

Without further approximations, one may now use (2.20) to obtain

$$Q_1(1)=\left[d_0-\Delta R_1-R_1\int d^3r'\frac{e^{-r'/\xi}}{r'}\rho_{\rm cr}(r',R_1)\right]$$
$$+\frac{R_1}{\xi}Q_1(1)\ . \tag{2.29}$$

To order $(\phi)^{1/2}$ this becomes

$$Q_1(1)=\left[d_0-\Delta R_1-R_1\int d^3r'\frac{e^{-r'/\xi}}{r}\rho_{\rm cr}(r',R_1)\right]$$
$$\times\left[1+\frac{R_1}{\xi}\right]\ . \tag{2.30}$$

The two-particle charge is

$$Q_1(2,1)=Q_1(1)-R_1\frac{e^{-r/\xi}}{r}Q_2(2)$$
$$-R_1\int d^3r'\frac{e^{-r'/\xi}}{r}\rho_{\rm cr}(\mathbf{r}-\mathbf{r}',R_2)\ . \tag{2.31}$$

These equations give closed expressions for the dynamics of the one- and two-point correlation functions to order $(\phi)^{1/2}$. The term in the first set of large parentheses of (2.30) has a natural physical interpretation. The average charge on a single particle is first the charge it would have in the absence of any interactions $d_0-\Delta R_1$. Then one must subtract the effect of interactions. We have seen that a potential Φ_∞ induces a charge $-R_1\Phi_\infty$ on a particle of size R_1. One integrates over all locations the screened potential due to charge fluctuations and multiplies by R_1. This gives the second term in the first set of large parentheses.

Let us now leave the terminology of electrostatics and rewrite these expressions directly in terms of particle growth rates. The growth rate of a single particle, when all others have been averaged over, is

$$v_1(R_1)=\frac{D}{R_1}[\Delta_1(1)-d_0/R_1]\ , \tag{2.32a}$$

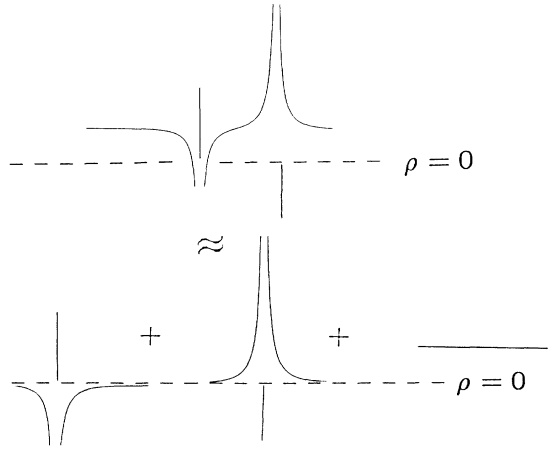

FIG. 4. Correlations up to order $(\phi)^{1/2}$ may be included by approximating the charge distribution surrounding two interacting point charges by the sum of distributions that would surround them were they well separated.

where

$$\Delta_1(1)=\Delta\left[1+\frac{R_1-d_0/\Delta}{\xi}+\int d^3r'\frac{e^{-r'/\xi}}{r}\rho_{\rm cr}(r',R_1)\right] . \tag{2.32b}$$

Similarly, a pair of particles growing in an averaged background obeys

$$v_1(R_1,R_2,r,t)=\frac{D}{R_1}[\Delta_1(1,2)-d_0/R_1] , \tag{2.33a}$$

with

$$\Delta_1(1,2)=\Delta_1(1)-\frac{e^{-r/\xi}}{r}\frac{v_2(2)}{D}R_2^2 +\Delta\int d^3r'\frac{e^{-r'/\xi}}{r'}\rho_{\rm cr}(|\mathbf{r}-\mathbf{r}'|,R_2) , \tag{2.33b}$$

$$\rho_{\rm cr}(r,R_1)=\int dR_2\frac{G_2^c(R_1,R_2,r)}{g_1(R_1,t)}Q_2(2) . \tag{2.27}$$

A similar expression holds for $v_2(1,2)$. The medium about each particle becomes polarized, as correlations develop, and it is the effect of this correlation cloud, described by $\rho_{\rm cr}$, that will spread the distribution function. The term $[R-(d_0/\Delta)]/\xi$ is independent of correlations and was first discovered by Marqusee and Ross.[31] The interesting problem remaining is to evaluate $g_2(R_1,R_2,r,t)$ and it is to that we now turn.

D. Calculation of correlations

The significance of $v_1(1,2)$ and $v_2(1,2)$ is that they describe the time evolution of the two-particle correlation function. Applying (2.15) to $g_2(R_1,R_2,r,t)$ gives

$$\frac{\partial}{\partial t}g_2(R_1,R_2,r,t)=-\sum_{k=1}^{2}\frac{\partial}{\partial R_k}[v_k(1,2)g_2(R_1,R_2,r,t)] . \tag{2.34}$$

Therefore, a knowledge of the dynamics of pairs of interacting particles in an effective field is equivalent to knowledge of the two-point distribution function. The length scale on which correlations are important is ξ. Two particles separated by a distance ξ will affect each other weakly; however, there are many such pairs, and they make the dominant contribution. One may see this by guessing that $\rho_{\rm cr}$ will have the spatial dependence given by (2.28), and noticing that the behavior of $\rho_{\rm cr}$ on the scale of ξ will dominate the integrals in (2.32) and (2.33) for large ξ. The strategy will be to look at the time evolution of pairs of distant interacting particles since these are the most important to understand. The expressions we obtain will break down for particles that are very close to one another; however, such pairs are unlikely and give a vanishing contribution as $\phi\to 0$.

Particles that are separated by a distance ξ perturb each others' growth only slightly. Consider the distinct particles 1 and 2, separated by a distance r. Define $\delta_1(R_1,R_2,r,t)$ to give the total reduction in size of particle 1 over time due to particle 2, and define $\delta_2(R_2,R_1,r,t)$ similarly. We will derive an expression for $g_2(R_1,R_2,r,t)$ that is valid to first order in δ_1 and δ_2. The starting point is the observation that $g_2(R_1,R_2,r,t)$ has an exact solution in terms of its characteristic curves. If one chooses a small area in R_1-R_2 space at $t=0$ and finds $g_2(S_1,S_2,0)dS_1dS_2$ particles in it, the same number of particles will be present in the time-evolved image of that area. To find how that area evolves, one must solve the pair of deterministic equations

$$\dot R_1=v_1(1,2) \quad\text{and}\quad \dot R_2=v_2(1,2) .$$

Denote the solutions of these equations by $R_1(S_1,S_2,t)$ and $R_2(S_2,S_1,t)$, suppressing the dependence on r. $S_1(R_1,R_2,t)$ and $S_2(R_1,R_2,t)$ give the sizes at $t=0$ of a pair of interacting particles now of size R_1 and R_2. To express $g_2(R_1,R_2,r,t)$ in terms of its characteristic curves, one writes

$$g_2(R_1,R_2,r,t)=g_2(S_1(1,2),S_2(1,2),0)\frac{\partial^2 S_1(1,2)S_2(1,2)}{\partial R_1R_2} . \tag{2.35}$$

We will expand about the characteristic curves of noninteracting particles. Those curves are the solutions of

$$\dot R_1=v_1(1) \quad\text{and}\quad \dot R_2=v_2(2) , \tag{2.36}$$

which I will denote by $R_1(S_1,t)$ and $R_2(S_2,t)$. Similarly, one has the inverse functions $S_1(R_1,t)$ and $S_2(R_2,t)$. The expression for δ_1 in terms of these functions is precise but rather cumbersome. Given particles of radii R_1 and R_2 at time t, we know that at $t=0$ they had sizes $S_1(1,2)$ and $S_2(1,2)$. If they did not interact, they would have sizes $R_1(S_1(1,2),t)$ and $R_2(S_2(1,2),t)$ at time t. Therefore,

$$\delta_1(R_1,R_2,r,t)=R_1(S_1(1,2),t)-R_1 ,$$

and a similar expression holds for δ_2. From the definition of δ_1 it follows that

$$S_1(R_1,R_2,t)=S_1(R_1+\delta_1)\approx S_1(R_1)+\frac{\partial S_1(1)}{\partial R_1}\delta_1 , \tag{2.37}$$

to first order in δ_1. In order to use (2.37), recall that particles are assumed to be uncorrelated at $t=0$, so that

$$g_2(S_1,S_2,r,0)=g_1(S_1,0)g_1(S_2,0) . \tag{2.38}$$

In addition, the one-particle distribution function is given in terms of its characteristics by

$$g_1(R_1,t)=g(S_1(R_1),0)\frac{\partial S_1(1)}{\partial R_1} . \tag{2.39}$$

Placing (2.37) into (2.38), with the corresponding expression for $S_2(1,2)$, and working to first order in δ_1 and δ_2 I now obtain

$$G_2^c(R_1,R_2,r,t) =\sum_{k=1}^{2}\frac{\partial}{\partial R_k}[g_1(R_1,t)g_1(R_2,t)\delta_1(R_1,R_2,r,t)] . \tag{2.40}$$

This equation may be put in the form

$$g_2(R_1,R_2,r,t)dR_1dR_2=\prod_{k=1}^{2} g_1(R_k+\delta_k,t)d(R_k+\delta_k) , \tag{2.41}$$

which shows that the two-particle distribution function is simply a product of one-particle functions that have been displaced by an amount δ_k.

The computation of the two-particle correlation function is therefore reduced to a calculation of δ_1 and δ_2. It is first useful to have a very simple expression for these that will make possible simple estimates. To obtain one, write from (2.32) and (2.33) that

$$\dot{\delta}_1(R_1,R_2,r,t)\approx\frac{R_2^2 v_2(2)}{R_1}\frac{e^{-r/\xi}}{r} . \tag{2.42}$$

I have simply ignored the correlation cloud that is described by the last term on the right-hand side of (2.33b). In addition, one here treats the effect of particle 2 as though it develops linearly, although in fact it affects the size of particle 1 in a very nonlinear way. A rough time integration, which ignores the time dependence in several of the terms of (2.42), now gives

$$\delta_1(R_1,R_2,r,t)\approx\frac{e^{-r/\xi}}{r}\frac{[R_2^3-S_2^3(2)]}{3R_1} . \tag{2.43}$$

It is possible to improve on this expression. The calculation involves numerous approximations that are neither especially well controlled nor elegant; however, the final results have not depended on various different versions I have tried, although multiplicative coefficients have varied on the order of 10%. This is no more than a peculiar self-consistent problem in classical mechanics, and intuition can provide considerable help in guiding one to reasonable approximations. Details are contained in Appendix B; here is recorded only the final result which is

$$\delta_1(R_1,R_2,r,t)=\frac{\tilde{g}(R_1,t)}{g_1(R_1,t)}\left[\frac{e^{-r/\xi(t)}}{r}\frac{R_2^3-S_2^3(2)}{3\langle R\rangle}-\frac{Dt}{\langle R\rangle}\int d^3r'\frac{e^{-|\mathbf{r}-\mathbf{r}'|/\xi(t)}}{|\mathbf{r}-\mathbf{r}'|}\int d^3r'\rho_{\rm cr}(r',R_2)\right] , \tag{2.44}$$

with

$$\tilde{g}(R_1,t)=\frac{\langle R\rangle}{t}\int_0^t dt'\frac{g_1(R_1(S_1,t'),t')}{\bar{R}_1^1(t')}\frac{e^{-(\phi)^{1/2}\langle R\rangle/R_1}}{e^{-(\phi)^{1/2}\langle R\rangle/R_1(S_1,t')}} . \tag{2.45}$$

S_1 is here $S_1(R_1,t)$, the initial size of a noninteracting particle that will be of size R_1 at time t. Using this expression in (2.40), placing the result in (2.27), and solving self-consistently gives

$$\frac{\partial}{\partial t}g_1(R_1,t)=-\frac{\partial}{\partial R}[v_{\rm eff}(R_1,t)g_1(R_1,t)]+\frac{\partial}{\partial R_1}\mathcal{M}(R_1,t)\frac{\partial}{\partial R_1}\tilde{g}(R_1,t) , \tag{2.46a}$$

with

$$v_{\rm eff}=\frac{D}{R_1}\left[\Delta\left[1+\alpha(t)\langle\tilde{g}/g\rangle\frac{R_1^3-S_1^3(1)}{3\langle R\rangle^2\xi}+\frac{R_1-\frac{d_0}{\Delta}}{\xi}\right]-\frac{d_0}{R_1}\right] , \tag{2.46b}$$

$$\mathcal{M}(R_1,t)=\alpha(t)\frac{D\Delta}{R_1}\frac{\left\langle[R_2^3-S_2^3(2)]\left[R_2-\frac{d_0}{\Delta}\right]\right\rangle}{3\xi\langle R\rangle^2} , \tag{2.46c}$$

and

$$\alpha(t)=\frac{1}{1+(1+x)^{1/2}} , \tag{2.46d}$$

where

$$\langle\tilde{g}/g\rangle=\int\frac{dR_1}{n}\tilde{g}(R_1,t) ,$$

and

$$x=\langle\tilde{g}/g\rangle\frac{Dt\,\Delta}{\langle R\rangle^2} .$$

In this manner, the continuity equation becomes a second-order equation. The second derivative term in (2.46a) has its origin in Eq. (2.40). The result looks like a diffusion equation; however, its physical significance is different from that of a diffusion equation since in the model considered to this point, there are no random forces acting on short-time scales. Although we are averaging over an ensemble of initial conditions, our system is essentially deterministic; nonetheless, one must solve a second-order parabolic equation to discover how it behaves. For (2.46) to make sense, the coefficient $\mathcal{M}$ must be positive. In all numerical work, this has been true.

III. COMPARISON WITH EXPERIMENTS, SIMULATIONS, AND PREVIOUS THEORIES

A. Experiments

For references to the experimental literature on particle coarsening one may consult the review articles already mentioned,[14,33] and a particularly comprehensive article, although only including experiments until 1972, by Fischmeister and Grimvall.[34] Most experiments seem tru-

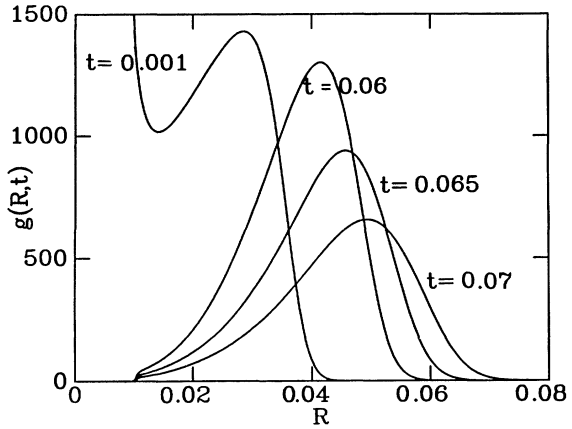

FIG. 5. The development of particle size distributions is shown following a fairly deep quench. The final volume fraction equals 0.05. At the earliest time, $t=0.001$, nucleation is in progress. Thereafter the distribution settles into its asymptotic form. The distribution function falls to zero at $R=0.01$ because of the way that nucleation is included in the theory; see Ref. 28.

ly to have reached the late stage. In Figs. 5 and 6 are shown two representative time sequences that result from a numerical simulation of the process of nucleation and growth. Details on how nucleation is included in the calculation may be found in Ref. 28. Once nucleation ends, the curves result from a numerical solution of Eq. (2.46). The important point is that immediately following nucleation, distribution functions become quite narrow, and they broaden only when they reach the late asymptotic stage of growth. Therefore, anomalously broad distributions cannot be explained as transients, and experimental distributions that are very broad must be in the asymptotic regime. In Fig. 6 appears a peculiar double-humped transient. Such a structure occurs only following a slow nucleation process, after a period in which many well-separated particles have been growing without competing with one another, never after spinodal decomposition. There is no experimental evidence for or against the effect. The mathematical origin of this peculiar intermediate structure is in the fact that the second-derivative term of (2.46a) is retarded in time; but it has a physical interpretation as well. Groups of particles have been growing freely and now enter into competition. If one looks at any pair of particles within a correlation length ξ, he will see that one member of the pair is larger than the other. Once the particles begin to compete, the larger will grow at the expense of the smaller, and since the two were not long ago almost the same size, the victor in this competition will shoot far ahead, while the loser rapidly shrinks to nothing. The distribution splits into two groups, one of losers, one of winners, and only when the large group of losers disappears does the distribution approach the steady state.

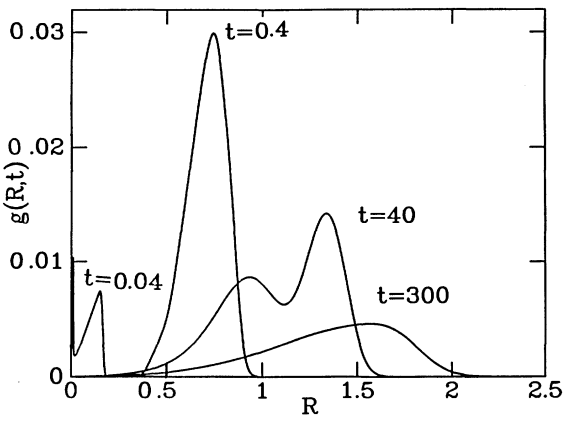

FIG. 6. The development of particle size distributions following a fairly shallow quench. The final volume fraction ϕ_f equals 0.05. At $t=0.04$ (scaled time) nucleation is in progress with the distance along the R axis scaled so that $d_0/\Delta(0)=0.01$. Since the quench has been shallow, a period of free growth follows nucleation lasting from $t\sim 0.2$ until $t\sim 15$. Correlations then become active and produce a striking bimodal transient. By $t\sim 100$ the transient has vanished and the distribution appears to have entered the asymptotic regime. However, the variance of the scaled distribution will continue to increase until $t\sim 4000$. At first the distribution resembles the distribution of Lifshitz and Slyozov, only gradually becoming broader.

With two exceptions[35,36] all coarsening experiments have been in alloy systems. Two methods have been used to obtain the distributions, direct counting of droplets, and an analysis of small-angle x-ray scattering data. Magnetic measurements are sometimes used to determine the volume fraction of precipitate and average particle size.[37,4] The first method is most reliable. One takes a section of material and, perhaps following additional treatment, places it beneath a microscope, counts the droplets, and measures. The tedium of the procedure may account for the very poor resolution of most experiments. The best one of which I am aware was performed by Bower and Whiteman[5] in an iron, silicon, and titanium alloy. Later investigators[6] claim that the precipitates which develop in that system are Fe_2SiTi and that their growth is limited by the diffusion of titanium. Since growth is limited by the diffusion of a single component, the theory given here should apply. The system is a good one because lattice mismatch between the precipitate grains and the iron background is minimal, and the lattice structure of the grains remains coherent with that of the matrix until they reach a size of approximately 1300 Å. The volume fraction of precipitate is around five percent. In Fig. 7 are superposed data from this experiment at two different times. Between the two examinations, the average particle size increased by a factor of 4, and since the scaled distributions do not change during this time, the samples are certainly in the asymptotic region. In addition are included some data of Rastogi and Ardell,[4] and Seno *et al.*[7] since these experiments were also conducted at five percent volume fraction. The experiment of Seno *et al.* agrees more closely with the curve of Lifshitz and Slyozov than with my prediction. However, the time sequence these authors present shows that the particle size distributions are continuing to broaden, and $R\sim t^{1/5}$, so they may well be seeing intermediate-stage behavior of the

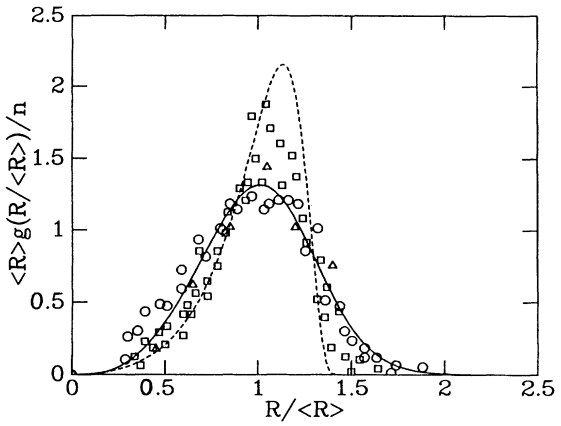

FIG. 7. The theory of Sec. II, the solid line, is compared with the prediction of Lifshitz and Slyozov, the dashed line, and with three experiments at 5% volume fraction. The circles represent the data of Bower and Whiteman, Ref. 5, which I believe to be the most careful experiment yet conducted. The data of Seno *et al.*, Ref. 7, in Cu-Co (squares) probably come from the intermediate stage. The triangles represent the data of Rastogi and Ardell in Ni-Si, Ref. 4.

type appearing in Fig. 6. In Fig. 8 are superposed data from three experiments[7,9] conducted at one percent volume fraction. The agreement between theory and experiment remains plausible, although it is by no means conclusive. The sharply peaked distribution is again due to Seno *et al.*[7] Finally, in Fig. 9 are superposed the results of several experiments[10,12] at ten percent volume fraction and above fraction and above. Recall that the theory is only accurate to order $(\phi)^{1/2}$. If $\phi=0.1$, then ϕ and $(\phi)^{1/2}$ are of the same order of magnitude. Computer simulations to be discussed presently also suggest that the theory begins to fail at volume fractions of ten percent and above. Therefore, I have not included a comparison with the present theory upon this last graph, although the agreement would not be especially bad. Whether the agreement with experiment achieved at five percent is fortuitous is therefore not clear.

An interesting result of Eq. (2.46) is that one must descend to very low volume fractions in order to recover the results of Lifshitz and Slyozov. In Fig. 10(a) is shown the root-mean-square width of asymptotic distributions as a function of volume fraction. Even at volume fractions as low as $\phi=10^{-4}$ the effects of correlations are noticable. Notice that I do not converge perfectly to the asymptotic result of Lifshitz and Slyosov at very low volume fraction, but only reach within 2% because limit time was available for the computing. The coefficient growth $\langle R\rangle^3/t$ depends upon volume fraction as shown in Fig. 10(b).

Some experiments use small-angle x-ray scattering to probe particle size distributions. In order to obtain the distributions from scattering data, one usually assumes that all particles are spatially uncorrelated.[38] In that case the scattering intensity is

$$I_1(k)=\int \frac{dR_1}{n} g_1(R_1,t)[F(R_1,k)]^2 ,$$

where $k \mid \mathbf{k}_{\text{incident}}-\mathbf{k}_{\text{scattered}} \mid$ and

$$F(R,k)=\frac{4\pi}{k^3}[\sin(kR)-kR\cos(kR)]$$

is the scattered amplitude due to a single spherical particle. However, as we now know the form of spatial correlations, we are in a position to examine the success of this assumption. I have checked that long-range correlations should be more important than short-range ones, and find that to order $(\phi)^{1/2}$ the scattering intensity should be

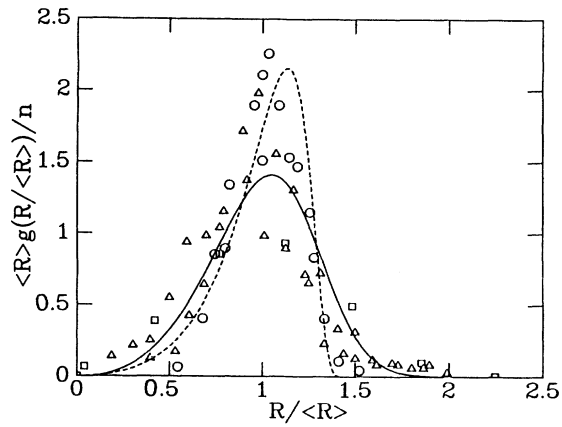

FIG. 8. The theory of Sec. II, the solid line, compared with the prediction of Lifshitz ane Slyzov, the dashed line, and with four experiments at 1% volume fraction. The agreement is not especially good but the experiments have not much resolution. The circles represent data of Seno *et al.*, Ref. 7, in Cu-Co, the triangles, Wirtz and Fine in MgO-Fe, Ref. 8, and the squares, Hirata and Kirkwood, Ref. 9, in Ni-Al.

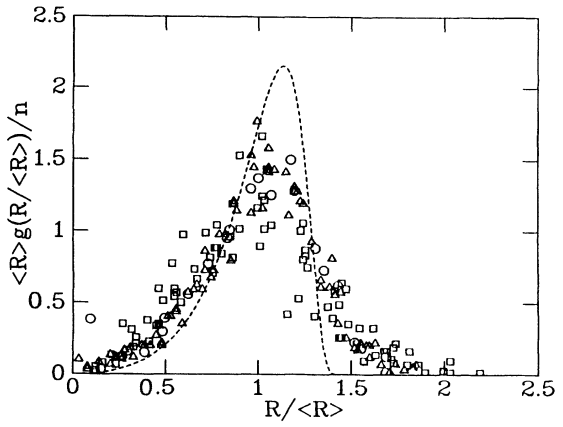

FIG. 9. These experiments, conducted at volume fractions of 10–60%, are compared with the theory of Lifshitz and Slyozov. The theory of Sec. II has certainly broken down at this high a volume fraction. The circles represent data of Chellman and Ardell, Ref. 10, in Ni-Al and Ni-Cr-Al, squares, Ardell and Nicholson in Ni-Al, Ref. 11, and triangles, Chaturvedi and Chung, Ref. 12, in Co-Ni-Cr-Ti.

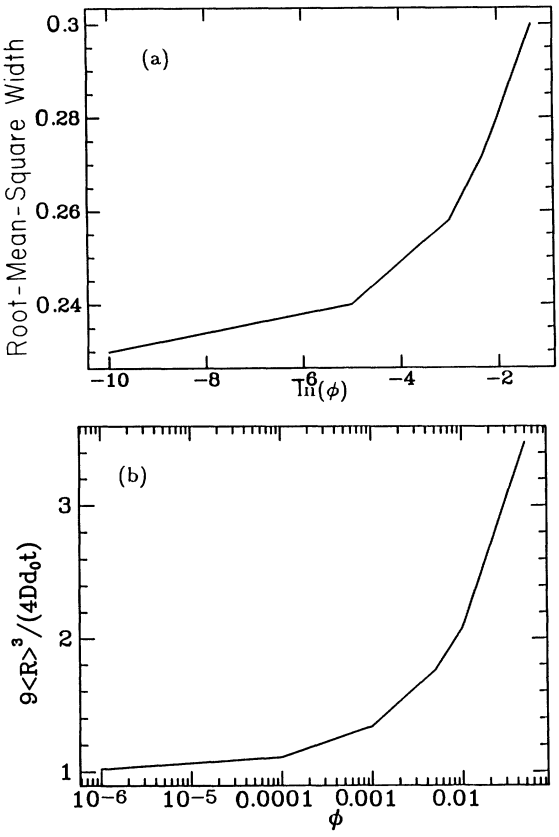

FIG. 10. One must go to very low volume fractions before the effects of correlations disappear. The root-mean-square width of asymptotic distributions is plotted as a function of volume fraction in (a). The limit at zero volume fraction should be a root-mean-square width of 0.215, which is not quite attained due to numerical inaccuracy. In (b) is shown the dependence of the rate constant $\langle R\rangle^2/t$ on volume fraction.

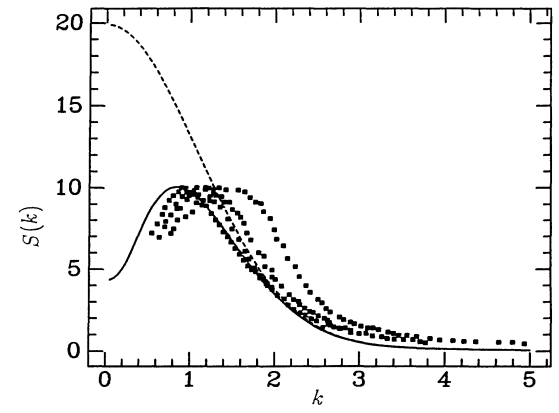

FIG. 11. Equation (6.10) predicts that scattering data should resemble the solid line; without correlations between particles, the same collection of particles would produce the dashed line. Superposed are the scattering data of Pahl and Cohen, Ref. 40; the vertical scale is chosen so that peaks of theory and experiment match. Notice that to deduce the particle size distribution from these data under the assumption that particles are uncorrelated would be very risky.

$$I\sim I_1(k)-I_2(k)\ ,$$

$$I_2(k)=\tfrac{2}{3}\int \frac{dR_1}{n}\frac{dR_2}{n}\frac{1}{1+(k\xi)^2}\frac{1}{1+x+(\xi k)^2}\frac{\tilde{g}(R_1,t)}{\langle R\rangle^2}$$
$$\times[A_1(k,1,2)-A_2(k,1,2)]\ , \tag{3.31}$$

with

$$A_1(k,R_1,R_2)$$
$$=\frac{\partial}{\partial R_1}F(R_1,k)F(R_2,k)g_1(R_2)R_2^3[(k\xi)^2+1]\ ,$$

and

$$A_2(k,R_1,R_2)=\frac{\partial}{\partial R_1}F(R_1,k)\frac{\partial}{\partial R_2}F(R_2,k)$$
$$\times\tilde{g}(R_2,t)\frac{x}{\langle\tilde{g}/g\rangle}\left\langle R^4-R^3\frac{d_0}{\Delta}\right\rangle\ .$$

The quantities x and $\langle\tilde{g}/g\rangle$ have been defined after (2.46). Using the numerical solutions of (2.46) we are now in a position to calculate the scattering intensities that an experiment should produce. In Fig. 11 is shown the result at 5% volume fraction. The solid line includes the correlations according to (3.1), and the dashed line shows how the scattering intensity would change if particles were spatially uncorrelated. These curves are sufficiently different so that I find it difficult to believe one could accurately reconstruct particle size distributions from the solid line, assuming the particles to be dispersed at random. Data from a scattering experiment[39,40] are also shown, exhibiting the structure one expects for correlated particles. Unfortunately, the shape of the scattering curve near $k=0$ depends sufficiently upon the approximations leading to (2.46) that I do not believe one can use scattering data to produce particle size distributions with any confidence.

B. Numerical simulations

A final technique that may be used to test the predictions of the theory embodied in Eqs. (2.46a)–(2.46d) is a direct computer simulation of the starting model contained in Eqs. (2.4)–(2.6). This is the purpose for which Weins and Cahn[15] originally formulated the model, but they run into numerical problems associated with the long-range interactions between particles. Voorhees and Glicksman[41,42] have improved upon the work of Weins and Cahn, but can study a system no larger than 200 particles, and therefore are in no position to study the development of correlations. As particles disappear, they create new spatial configurations at random, thus destroying whatever spatial correlations have developed. One result is that their particle size distributions seem less broad than those seen experimentally at low volume fraction. A more successful simulation has recently been carried out by Beenakker[43] at 10% volume fraction. Equation (2.6) is inverted only approximately; the most worrisome result of his approximations is a drift in the volume fraction of precipitate during the simulation, although one starts so far

into the asymptotic regime that no change in volume fraction should be observable. He has measured certain moments of the two-particle correlation function, and these are compared with the results of the present theory in Fig. 12. The theory relies upon the separation of length scales $\langle R \rangle \ll \xi$ and this inequality is clearly not satisfied at volume fractions of ten percent. For large R, $R/\langle R \rangle > 2$, the theory describes the correlation functions correctly, but for smaller R it breaks down. By way of comparison, Fig. 12 also shows the correlations that would develop among spheres placed down with no interactions but hard sphere repulsion. The distribution function obtained by Beenakker is not quite so broad as the present theory would predict, and is similar to those seen experimentally. Contributions of order ϕ have become important at this volume fraction.

None of the simulations carried out so far have been capable of studying intermediate-stage behavior, for they required from the outset $\sum Q_i = 0$, which is characteristic of the very late stages of growth only, as discussed following Eq. (2.24). A simulation which can study the full time-dependent behavior of the system following nucleation might be carried out in the following way. It is very difficult directly to invert Eq. (2.6). But we may simplify it. Rewrite the equation as

$$Q_i = d_0 - R_i \left[\Phi_\infty + \sum_{\substack{i,j \\ (i \neq j)}} \frac{e^{-|\mathbf{r}_i - \mathbf{r}_j|^2/2l^2}}{|\mathbf{r}_i - \mathbf{r}_j|} \langle Q \rangle \right] - R_i \sum_{j(\neq i)} (Q_j - \langle Q \rangle) \frac{e^{-|\mathbf{r}_i - \mathbf{r}_j|^2/2l^2}}{|\mathbf{r}_i - \mathbf{r}_j|} . \tag{3.2}$$

Since l is much greater than the interparticle spacing,

$$\sum_{\substack{i,j \\ (i \neq j)}} \frac{e^{-|\mathbf{r}_i - \mathbf{r}_j|^2/2l^2}}{|\mathbf{r}_i - \mathbf{r}_j|} \approx 4\pi n l^2 .$$

In addition, as pointed out and investigated by Beenakker,[44] particles much farther away than the screening distance from particle i should not contribute to the last sum in (3.2). Using (2.7) one can expect that (3.2) is equivalent to

$$Q_i = d_0 - R_i \Delta - \sum_{j \in S_i} (Q_j - \langle Q \rangle) \frac{R_i}{|\mathbf{r}_i - \mathbf{r}_j|} . \tag{3.3}$$

S_i is the set of droplets within a few screening lengths of particle i. This is now a sparse matrix equation and can quickly be inverted. My own attempts to use this approach have been unsuccessful with systems larger than 600 particles, but more progress should be possible.

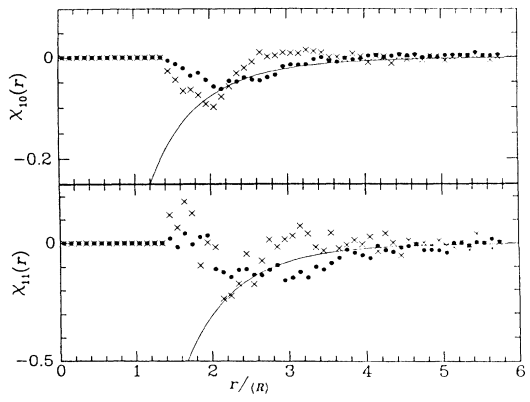

FIG. 12. Beenakker, Ref. 43, has measured two moments of the two-point correlation functions, and the solid circles compare the results to the correlations that would develop among the hard spheres, shown as crosses, and to my theory the solid line. All hard sphere exclusions are of order ϕ and the theory neglects them, but at 10% volume fraction, where this simulation was carried out, they are clearly as important as the longer-range correlations. The correlation functions plotted are described by

$$\chi_{nm} = \langle (R_1/\langle R \rangle - 1)^n (R_2/\langle R \rangle - 1)^m \rangle .$$

C. Previous theories

Most attempts to explain anomalously broad late-stage distributions have been phenomenological. They are well described in review articles by Voorhees[33] and by Tsumuraya and Miyata.[14] I am not convinced that any phenomenological theory captures the behavior of the system; in particular, none have guessed that the screening length ξ is of primary importance. The work of Marqusee and Ross[31] is the first to notice this length, although neglecting the effect of correlations. With the exception of the work of Venzl,[45] no theory of anomalous broadening before this one has chosen to look at time-dependent effects, although the time dependence of the equations of Lifshitz and Slyozov has been examined numerically, also by Venzl,[46] and Lifshitz and Slyozov[2] supplied an analytical time-dependent solution to their equations.

However, Tokuyama, Kawasaki, and Enomoto have carried out a systematic investigation of this problem before me and were the first[21] to calculate an expansion in powers of $\phi^{1/2}$ from a starting point nearly identical to Eq. (2.6). Their approach uses techniques of diagrammatic perturbation theory, and despite a recent simplification of the method,[22] it remains quite elaborate. To a certain point our treatments must be identical. In particular, the system of Eqs. (2.32) and (2.33) in this paper must have the same content as Eqs. (3.15) and (4.17) in Ref. 22, although I have not shown the equivalence directly.

As we have seen, the progression from (2.32) and (2.33) to tractable equations is not simple. The choices made by Enomoto, Kawasaki, and Tokuyama[24] to achieve this aim seem particularly uncontrolled, and involve eliminating all but derivatives of first and second order from a differential equation of infinite order, without the benefit of a small parameter. Whereas our final equations are of roughly similar form, all of the coefficients are entirely different, and the spreading produced by their theory is less than that produced by mine.[23] In Fig. 13 are shown the results of the present theory together with the prediction of Tokuyama and Kawasaki and two experiments at five percent volume fraction. The degree of spreading found by Tokuyama, Kawasaki, and Enomoto is typical of all the phenomenological theories, except that of Ardell.[47] The

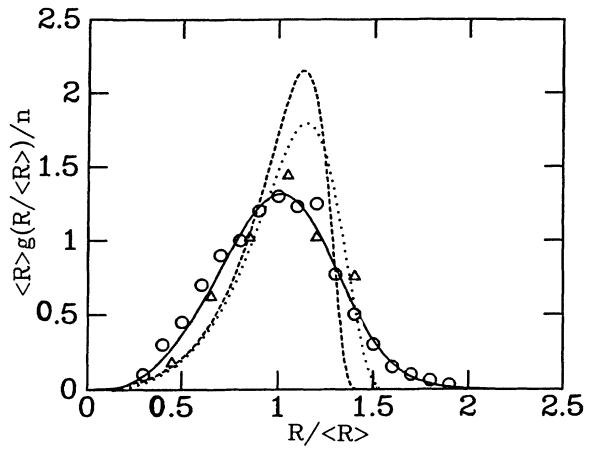

FIG. 13. The results of Enomoto, Tokuyama, and Kawasaki, Ref. 23 (dotted line), are compared with the curve of Lifshitz and Slyozov (dashed line), the present theory (solid line), the experiment of Bower and Whiteman, Ref. 5, and Rastogi and Ardell Ref. 4; all at 5% volume fraction. I have used only the drift term of Enomoto, Tokuyama, and Kawasaki, but Figs. 5, 6, and 7 of Ref. 23 show the numerical consequences of the neglected term to be small. The comparison is made at a low volume fraction, despite reasonable agreement with experiment at volume fractions as high as 50%, because I do not believe that our expansions are valid above volume fractions of 10%. Figure 12 shows how much the approximations of the present work have broken down at $\phi=0.1$, and Tokuyama, Kawasaki, and Enomoto are expanding in the same small parameter as I am. Many of their comparisons with experiment are at $\phi=0.35$, although they expand in $(3\phi)^{1/2}$, which has become larger than one.

difficulty has been to find a theory which accounts for the very flattened distribution function seen experimentally, without predicting wildly accelerated particle growth or other unphysical features; and in the present work that seems to have been accomplished. But the most important test of the conclusions of this paper would be an experimental measurement of the spatial correlations shown in Fig. 12. One should look for them in a system at 5% volume fraction or less. Perhaps in the future such experiments will be carried out.[48]

ACKNOWLEDGMENTS

I owe thanks to many people for criticism and encouragement during the completion of this work. J. S. Langer introduced me to the problem and pushed me hard to try to explain the solution clearly. C. Beenakker shared results in advance of publication. I have had especially useful comments from J. Deutsch, K. Kawasaki, A. Karma, M. Glicksman, P. Voorhees, and K. Binder. This work was supported by the U. S. Department of Energy under Grant No. DE-FG03-84ER45108 and the National Science Foundation under Grant No. PHY-82-17853, supplemented by funds from the U. S. National Aeronautics and Space Administration.

APPENDIX A: DO DROPLETS MOVE?

Whether droplet centers move in time, and how much, depends upon whether one considers droplets in a gas, fluid, or solid. Liquid droplets in a gas almost certainly are so buffeted by convective forces that it makes little sense to apply the theory of Sec. II.[49] Even solid droplets embedded in solid should move, and liquid droplets embedded in solid have been seen to move in time.[36] Let us consider droplets in a solid first. The main source of their motion is that material does not diffuse into a droplet at the same rate from all sides. The monopolar part of the diffusion field is what we have calculated so far. The dipolar part of the diffusion field should give the main contribution to the motion of the droplet. Let us ignore time dependent effects and consider solutions of

$$\nabla^2\Phi=0$$

subject to the boundary conditions (2.1) at the surface of the spheres in the system. Expand Φ in multipole moments in the following way:

$$\Phi(\mathbf{r})=\sum_i \frac{Q_i}{|\mathbf{r}-\mathbf{r}_i|}+\sum_i \frac{P_i\cdot(\mathbf{r}-\mathbf{r}_i)}{|\mathbf{r}-\mathbf{r}_i|^3}\ . \tag{A1}$$

Then the largest contribution to the center-of-mass motion of the ith sphere will be

$$\dot{r}_i=-\frac{DP_i}{R_i^3} \tag{A2}$$

along the direction of $\mathbf{P}$. A solution of Laplace's equation is

$$\Phi(\mathbf{r})=-\sum_i \int \frac{dS_i}{4\pi}\hat{\mathbf{n}}_i\cdot\frac{\nabla\Phi(\mathbf{r}')}{|\mathbf{r}-\mathbf{r}'|}\ , \tag{A3}$$

where $\hat{\mathbf{n}}_i$ is the outward normal to the ith sphere, and the integral is taken over the surface of the ith sphere. Substituting (A1) into (A3) and retaining only the terms of leading order, I obtain

$$P_i=-\sum_j \frac{R_j^3 Q_i(\mathbf{r}_i-\mathbf{r}_j)}{|\mathbf{r}_i-\mathbf{r}_j|^3}\ . \tag{A4}$$

As a result, the ratio of the center-of-mass velocity of a droplet to its radial growth rate is

$$\dot{r}_i/\dot{R}_i=\left|\sum_j \frac{R_j^3(\mathbf{r}_i-\mathbf{r}_j)}{R_i\mathbf{r}_i-\mathbf{r}_j|^3}\right|\ . \tag{A5}$$

In a relatively isotropic sample, the contributions of distant particles to this sum should cancel; (A5) should be dominated by a few nearby particles, and at most be of order unity. In that case the center-of-mass motion of spheres is of order $\langle R(t)\rangle$ after time t. Since at low volume fraction the important interactions are between spheres separated by the typical distance ξ, if their centers move a distance on the order of $\langle R\rangle$ it will not matter.

When droplets are contained in a fluid the case is more complicated because droplets move more easily, have long-range hydrodynamic interactions, and are affected by gravity. These effects have been nicely discussed by Siggia.[50] Here we will simply see when to expect the correlations discussed in this paper to be destroyed by Brownian motion. A solid sphere of radius R will undergo Brownian motion governed by the effective diffusion constant

$$\mathcal{D}(R)\approx\frac{kT}{6\pi\eta R}\ , \tag{A6}$$

where η is the viscosity of the liquid, as

$$\delta\tau_{\rm rms}\sim[\mathcal{D}(R)t]^{1/2}\ . \tag{A7}$$

One may also write that the diffusion constant for monomers is

$$D\sim\frac{kT}{6\pi\eta\alpha}\ ,$$

where α is the radius of a monomer. Take α to be the constant[27] d_0/c_o^0; c_o^0 denotes the equilibrium concentration of the minority phase in the majority phase. In this case

$$\delta_{\rm rms}\sim\langle R\rangle/(c_o^0)^{1/2}\ . \tag{A8}$$

Therefore, Brownian motion of spheres in a fluid should be unimportant when $\phi\ll c_o^0$. Another way to view this problem is to add a term representing the diffusive effect of thermal fluctuations to Eq. (2.34). If the motion of sphere centers is allowed, that equation becomes

$$\frac{\partial}{\partial t}g_2(1,2)=-\sum_{k=1}^{2}\frac{\partial}{\partial R_k}[v_k(1,2)g_2(1,2)]+\mathcal{D}(\mu)\nabla^2 g_2(1,2)\ . \tag{A9}$$

Here μ is $R_1R_2/(R_1+R_2)$. One may now easily verify that if $\phi\ll c_o^0$ then the term just added is of order ϕ and may be neglected.

APPENDIX B: THE CALCULATION OF δ

The equation of motion for δ_1 is

$$\dot\delta_1(R_1,R_2,r,t)=v_1(R_1+\delta_1)-v_1(R_1,R_2,r,t)\ . \tag{B1}$$

Total time derivatives are time derivatives in which initial conditions are held fixed:

$$\dot\delta_1=\left.\frac{\partial\delta_1}{\partial t}\right|_{s_1,s_2}\ .$$

Equation (B1) is a complicated nonlinear expression, and I do not know how to solve it exactly. We shall proceed by expanding in powers of δ_k, but this procedure is not entirely satisfactory. Using the expressions (2.32) and (2.33), we find

$$\dot\delta_1(1,2)=v_1(R_1+\delta_1)-v_1(R_1)+\frac{e^{-r/\xi}}{r}\frac{(R_2)^2}{R_1}v_2(1,2)-\frac{D}{R_1}\int d^3r'\frac{e^{-|\mathbf{r}-\mathbf{r}'|/\xi}}{|\mathbf{r}-\mathbf{r}'|}\rho_{\rm cr}(r',R_2)\ . \tag{B2}$$

So long as δ_1 is much smaller than R_1, one may safely write

$$v_1(R_1+\delta_1)-v_1\approx\frac{\partial}{\partial R_1}v_1(1)\delta_1(1,2)\ . \tag{B3}$$

However, this expansion always breaks down for sufficiently small R_1; first because R_1 can be chosen as small as desired (although it should be larger than d_0/Δ), and second because particles shrink with accelerating rapidity when they become smaller than the critical radius. A small size difference between shrinking particles magnifies rapidly and δ_1 will become large, typically of order $(d_0/\Delta(0))(\phi)^{1/2}$ by the time particles become very small. In general, particles much smaller than the critical radius are uninteresting, they are disappearing rapidly and the precise rate at which they do it should not be very unimportant. That the expansion (B3) breaks down for small R_1 will not be important if later work does not depend on the result of the expansion where it is bad. But even this is not the case; use of (B3) would lead to the conclusion that δ_1 becomes infinite for small R_1, which is clearly unphysical, and subsequent results would depend upon the unphysical region. I have found no satisfying way to cure this defect, and have settled upon the strategy of adding a term of order ϕ which has no effect for $R_1\sim\langle R\rangle$ but eliminates the unphysical behavior for small R_1. One expects the solution of

$$\dot\delta=\frac{\partial v_1(1)}{\partial R_1}\delta$$

to grow exponentially for small R, where $v_1(1)$ becomes very large. A better approximation to

$$\dot\delta=v(R+\delta)-v(R)$$

results by including a quadratic term to stabilize the divergence at small radii:

$$\dot\delta=\delta\frac{\partial v}{\partial R}+\frac{\partial^2 v}{\partial R^2}\delta^2/2\ ;$$

however, here no analytical solution is available. Therefore, I will add to the right-hand side of (B3) the term

$$(\phi)^{1/2}\langle R\rangle\delta_1(1,2)\frac{v_1(R_1)}{R_1^2}\approx-\delta_1(1,2)\frac{d}{dt}(\phi)^{1/2}\langle R\rangle\frac{1}{R_1}\ .$$

For small R_i, this term is of the same order as

$$\frac{\partial^2 v}{\partial R^2}\delta^2/2\ ,$$

since $\delta\sim\langle R\rangle(\phi)^{1/2}$ for small R. For $R_1\sim\langle R\rangle$ the term is very small, and since it is formally of order ϕ, one has the freedom to add or subtract it as one pleases. That it becomes infinite for small R_1 indicates that the expansion

in powers of $(\phi)^{1/2}$ has broken down, but it is chosen to be physically sensible, and no final results will depend on the particular form I have chosen.

Since the continuity equation may be written

$$\frac{dg_1}{dt} = -g_1(R_1,t)\frac{\partial v_1(1)}{\partial R_1} ,$$

one may write a solution for δ_1 in the form

$$\delta_1(R_1,R_2,r,t) = \int_0^t dt' \frac{g_1(R_1(S_1,t'),t')}{g_1(R_1,t)} \frac{e^{-(\phi)^{1/2}\langle R\rangle/R_1}}{e^{-(\phi)^{1/2}\langle R\rangle/R_1(S_1,t')}} \times \left[\frac{e^{-r/\xi}}{r} \frac{[R_2(S_2t')]^2}{\bar{R}_1^1(t')} v_2(R_2(S_2,t')) - \frac{D}{R_1} \int d^3r' \frac{e^{-|\mathbf{r}-\mathbf{r}'|/S(t')}}{|\mathbf{r}-\mathbf{r}'|} \rho_{cr}(r',R_2(S_2,t')) \right] .$$

in order to put this expression into usable form, the following three more approximations are necessary.

(1) Regard the time integral as a time average, and replace the average of products by a product of averages in such a way as to express δ_1 in the form $f_1(R_1,t)f_2(R_2,t)$. This step is necessary if the final results are to be numerically tractable.

(2) Evaluate $e^{-r/\xi(t')}$ at t, somewhat overstating the range of correlations. This approximation is sensible since the time averages are dominated by recent times. It is not obvious that recent times are most important, but scaling fails unless it is true and all of my numerical confirm the hypothesis. At this point we have

$$\delta_1(R_1,R_2,r,t) = \frac{\tilde{g}(R_1,t)}{g_1(R_1,t)} \left[\frac{e^{-r/\xi(t)}}{r} \frac{R_2^3 - S_2^3(2)}{3\langle R\rangle} - \frac{D}{\langle R\rangle} \int d^3r' \frac{e^{-|\mathbf{r}-\mathbf{r}'|/\xi(t)}}{|\mathbf{r}-\mathbf{r}'|} \int dt' \int d^3r' \rho_{cr}(r',R_2(S_2,t')) \right] ,$$

with

$$\tilde{g}(R_1,t) = \frac{\langle R\rangle}{t} \int_0^t dt' \frac{g_1(R_1(S_1,t'),t')}{\bar{R}_1^1(t')} \frac{e^{-(\phi)^{1/2}\langle R\rangle/R_1}}{e^{-(\phi)^{1/2}\langle R\rangle/R_1(S_1,t')}} .$$

We may substitute $S_2(2)$ for $S_2(1,2)$ since these two functions differ only to order $(\phi)^{1/2}$, and within an expression already of that order, the difference is negligible.

(3) The time average of ρ_{cr} is impossible to evaluate unless it is done iteratively. Here I will simply set the time average of ρ_{cr} equal to its value at time t, again invoking the notion of scaling to argue that recent times must be the most important. I have also tried multiplying by a constant, chosen so that the time integral of a certain moment of ρ_{cr} is chosen correctly, but as the value of this constant turns out to be 1.2, and it ends up inside a square-root sign, I will omit it here. This fact alone indicates that the terms appearing in the final answer should not be taken seriously beyond an accuracy of $\sim 10\%$. Finally,

$$\delta_1(R_1,R_2,r,t) = \frac{\tilde{g}(R_1,t)}{g_1(R_1,t)} \left[\frac{e^{-r/\xi(t)}}{r} \frac{R_2^3 - S_2^3(2)}{3\langle R\rangle} - \frac{Dt}{\langle R\rangle} \int d^3r' \frac{e^{-|\mathbf{r}-\mathbf{r}'|/\xi(t)}}{|\mathbf{r}-\mathbf{r}'|} \int d^3r' \rho_{cr}(r',R_2) \right] .$$

*Present address: James Franck Institute, University of Chicago, IL 60637.

[1]I. M. Lifshitz and V. V. Slyozov, Zh. Eksp. Teor. Fiz. **35**, 479 (1958) [Sov. Phys.—JETP **8**, 331 (1959)]; J. Phys. Chem. Solids **19**, 35 (1961).

[2]I. M. Lifshitz and V. V. Slyozov, Soviet Phys. Solid State **1**, 1285 (1960).

[3]A. J. Ardell, *The Mechanism of Phase Transformations in Crystalline Solids* (Institute of Metals, London, 1969), p. 111.

[4]P. K. Rastogi and A. J. Ardell, Acta. Metall. **19**, 321 (1971).

[5]E. N. Bower and J. A. Whiteman, *The Mechanism of Phase Transformations in Crystalline Solids* (Institute of Metals, London, 1969), p. 119.

[6]D. H. Jack and R. W. K. Honeycombe, Acta. Metall. **20**, 787 (1972).

[7]Y. Seno *et al.*, Trans. Jpn. Inst. Metals **24**, 491 (1983).

[8]G. P. Wirtz and M. E. Fine, J. Am. Ceram. Soc. **51**, 402 (1968).

[9]T. Hirata and D. H. Kirkwood, Acta. Metall. **25**, 1425 (1977).

[10]D. J. Chellman and A. J. Ardell, Acta. Metall. **22**, 577 (1974).

[11]A. J. Ardell and R. B. Nicholson, J. Phys. Chem. Solids **27**, 1793 (1966).

[12]M. Chaturvedi and D. W. Chung, J. Inst. Metals **101**, 253 (1973).

[13]W. Ostwald, *Grundriss, der Allgem. Chemie* (Macmillan, London, 1908); p. 96, *Foundations of Analytic Chemistry*, 3rd English ed. (Macmillan, London, 1908), p. 22; *Principles of Inorganic Chemistry* (Macmillan, London, 1902), p. 258.

[14]K. Tsumuraya and Y. Miyata, Acta. Metall. **31**, 437 (1983).

[15]J. J. Wiens and J. W. Cahn, in *Sintering and Related Phenomena*, edited by G. C. Kuczynski (Plenum, London, 1973), p. 151.

[16]J. Friedel, *Dislocations* (Pergamon, London, 1964), Chap. XIV.

[17]F. R. N. Nabarro, in *The Physics of Metals*, edited by P. B. Hirsch (Cambridge University Press, Cambridge, 1975), Vol. 2, Chap. 4.

[18]A. Kelly, *Strong Solids* (Oxford University Press, London, 1973), Sec. 4.3.2, p. 130.
[19]M. Marder, Phys. Rev. Lett. **55**, 2953 (1985).
[20]K. Kawasaki and T. Ohta, Physica **118A**, 175 (1983).
[21]M. Tokuyama and Kawasaki, Physica **123A**, 386 (1984).
[22]K. Kawasaki, Y. Enomoto, and M. Tokuyama, Physica **135A**, 426 (1986).
[23]Y. Enomoto, M. Tokuyama, and K. Kawasaki, Acta Metall. **34**, 2119 (1986).
[24]M. Tokuyama, Y. Enomoto, and K. Kawasaki (unpublished).
[25]Thomson, Proc. R. Soc. Edinburgh **7**, 63 (1870).
[26]J. W. Gibbs, *The Scientific Papers of J. Willard Gibbs* (Dover, New York, 1961), Vol. 1, p. 229.
[27]E. M. Lifshitz and L. P. Pitaevskii, *Physical Kinetics* (Pergamon Press, Oxford, 1982). A common expression for d_0, when the minority phase is very dilute in the majority phase is $d_0 = 2\sigma c_o^0 v / kT(\Delta c)^2$, where σ is the surface tension, c_o^0 is the equilibrium concentration of the minority component in the majority phase, v is the volume per atom, k is Boltzmann's constant, and Δc, is the miscibility gap.
[28]M. Marder, Ph.D. thesis, University of California at Santa Barbara, 1986 (unpublished).
[29]P. W. Voorhees and G. B. McFadden (unpublished).
[30]C. Zener, J. Appl. Phys. **20**, 950 (1949).
[31]J. A. Marqusee and J. Ross, J. Chem. Phys. **80**, 536 (1984).
[32]C. Wagner, Z. Elektrochem. **65**, 581 (1961).
[33]P. W. Voorhees, J. Stat. Phys. **38**, 231 (1985).
[34]H. Fischmeister and G. Grimvall, in *Sintering and Related Phenomena,* edited by G. C. Kuczynski (Plenum, London, 1973).
[35]M. Kahlweit, Z. Phys. Chem. **36**, 292 (1963).
[36]P. W. Voorhees and R. J. Schaefer (unpublished).
[37]F. E. Luborsky, J. Phys. Chem. **61**, 1336 (1957).
[38]O. Glatter, in *Small-Angle X-Ray Scattering,* edited by O. Glatter and O. Kratky (Academic, London, 1982), p. 147.
[39]R. G. Pahl and J. B. Cohen, Scr. Metall. **18**, 397 (1984).
[40]R. G. Pahl and J. B. Cohen, Metall. Trans. **A15**, 1519 (1984).
[41]P. W. Voorhees, Ph.D. thesis, Rensselaer Polytechnic Institute, 1982 (unpublished).
[42]P. W. Voorhees and M. E. Glicksman, Metall. Trans. **A15**, 1081 (1984).
[43]C. Beenakker (unpublished).
[44]C. Beenakker and J. Ross (unpublished).
[45]G. Venzl, Phys. Rev. A **31**, 3431 (1985).
[46]G. Venzl, Ber. Bunsenges. Phys. Chem. **87**, 318 (1983).
[47]A. J. Ardell, Acta. Metall. **20**, 61 (1972).
[48]W. Casey (private communication).
[49]T. W. Peterson, F. Gelbard, and J. H. Seinfeld, J. Colloid Interface Sci. **63**, 426 (1977).
[50]E. D. Siggia, Phys. Rev. A **20**, 595 (1979).